

1 **Photonic Technologies for Quantum Information**  
2 **Processing**

3 **Prem Kumar,<sup>1,7</sup> Paul Kwiat,<sup>2</sup> Alan Migdall,<sup>3</sup> Sae Woo Nam,<sup>4</sup>**  
4 **Jelena Vuckovic,<sup>5</sup> and Franco N. C. Wong<sup>6</sup>**

5 *Received February 26, 2004; accepted May 6, 2004*

6 *The last several years have seen tremendous progress toward practical optical*  
7 *quantum information processing, including the development of single- and entan-*  
8 *gled-photon sources and high-efficiency photon counting detectors, covering a range*  
9 *of wavelengths. We review some of the recent progress in the development of these*  
10 *photonic technologies.*

11 **KEY WORDS:** Quantum dot; entanglement; down-conversion; single-photon  
12 detector.

13 **PACS:** 03.67.-a, 42.50.Dv, 42.65.Lm, 78.67.Hc, 85.60.Gz.

14 **1. INTRODUCTION**

15 It is now generally realized that fundamentally quantum-mechanical phe-  
16 nomena can enable significant, and in some cases, tremendous, improve-  
17 ment for a variety of tasks important to emergent technologies. Build-  
18 ing on decades of successes in the experimental demonstration of such  
19 fundamental phenomena, it is not surprising that photonics is playing a

<sup>1</sup>Departments of Electrical and Computer Engineering, and Physics and Astronomy, North-  
western University, Evanston, Illinois 60208-3118, USA. E-mail: kumarp@northwestern.edu

<sup>2</sup>Department of Physics, University of Illinois, Urbana-Champaign, Illinois 61801-3080,  
USA.

<sup>3</sup>Optical Technology Div., NIST, Gaithersburg, Maryland 20899-8441, USA.

<sup>4</sup>Quantum Electrical Metrology Division, NIST, Boulder, Colorado 80305-3328, USA.

<sup>5</sup>Department of Electrical Engineering, Stanford University, Stanford, California 94305,  
USA.

<sup>6</sup>Research Laboratory of Electronics, MIT, Cambridge, Massachusetts 02139, USA.

<sup>7</sup>To whom correspondence should be addressed. E-mail: kumarp@northwestern.edu



20 preeminent role in this nascent endeavor. Many of the objectives of quan-  
21 tum information processing are inherently suited to optics (e.g., quantum  
22 cryptography<sup>(1)</sup> and optical metrology<sup>(2)</sup>), while others may have a strong  
23 optical component (e.g., distributed quantum computing<sup>(3)</sup>). In addition,  
24 it is now known that, at least in principle, one can realize *scalable* lin-  
25 ear optics quantum computing (LOQC).<sup>(4)</sup> For these applications to attain  
26 their full potential, various photonic technologies are needed, including  
27 high fidelity sources of single and entangled photons, and high efficiency  
28 photon-counting detectors, both at visible and telecommunication wave-  
29 lengths. Much progress has been made on the development of these,  
30 though they are still not up to the demanding requirements of LOQC.  
31 Nevertheless, even at their present stage they have direct application to ini-  
32 tial experiments. Moreover, they may find use in various “adjacent” tech-  
33 nologies, such as biomedical and astronomical imaging, and low-power  
34 classical telecommunications. Here we describe a number of the leading  
35 schemes for implementing approximations of sources of single photons  
36 on-demand and entangled photons, followed by a review of methods for  
detecting individual photons.

## 38 2. SINGLE-PHOTON SOURCES

39 Photon-based quantum cryptography, communication, and computation  
40 schemes have increased the need for light sources that produce individual pho-  
41 tons. Ideally a single-photon source would produce completely characterized  
42 single photons on demand. When surveying attempts to create such sources,  
43 however, it is important to realize that there never has been and will never be  
44 such an ideal source. All of the currently available sources fall significantly  
45 short of this ideal. While other factors (such as rate, robustness, and complex-  
46 ity) certainly do matter, two of the most important parameters for quantifying  
47 how close a “single-photon source” approaches the ideal, are the fraction of  
48 the time the device delivers light in response to a request, and the fraction of  
49 time that that light is just a single photon.

50 In general single-photon sources fall into two categories—isolated quan-  
51 tum systems or two-photon emitters. The first type relies on the fact that a sin-  
52 gle isolated quantum system can emit only one photon each time it is excited.  
53 The trick here is obtaining efficient excitation, output collection, and good iso-  
54 lation of individual systems. The second type uses light sources that emit two  
55 photons at a time. Here the detection of one photon indicates the existence of  
56 the second photon. That knowledge allows the second photon to be manipu-  
lated and delivered to where it is needed.

## 58 2.1. Quantum Dot Single-Photon Sources

59 A quantum dot is essentially an artificial atom that is easily iso-  
60 lated so it is an obvious choice as the basis of a single-photon source.  
61 Single photons on-demand have been generated by a combination of  
62 pulsed excitation of a single self-assembled semiconductor quantum dot  
63 and spectral filtering.<sup>(5)</sup> When such a quantum dot is excited, either  
64 with a short (e.g., 3 ps) laser pulse, or with an electrical pulse,<sup>(6)</sup> elec-  
65 tron-hole pairs are created. For laser excitation, this can occur either  
66 within the dot itself, when the laser frequency is tuned to a reso-  
67 nant transition between confined states of the dot, or in the surround-  
68 ing semiconductor matrix, when the laser frequency is tuned above the  
69 semiconductor band gap. In the latter case, carriers diffuse toward the  
70 dot, where they relax to the lowest confined states. Created carriers recom-  
71 bine in a radiative cascade, leading to the generation of several photons  
72 for each laser pulse; all of these photons have slightly different frequen-  
73 cies, resulting from the Coulomb interaction among carriers. The last emit-  
74 ted photon for each pulse has a unique frequency, and can be spectrally  
75 isolated.

76 If the dots are grown in a *bulk* semiconductor material,<sup>(6)</sup> the  
77 out-coupling efficiency is poor, since the majority of emitted photons are  
78 lost in the semiconductor substrate. To increase the efficiency, an opti-  
79 cal microcavity can be fabricated around a quantum dot. An additional  
80 advantage is that the duration of photon pulses emitted from semiconduc-  
81 tor quantum dots is reduced, due to an enhancement of the spontaneous  
82 emission rate. This enhancement, also known as the Purcell factor, is pro-  
83 portional to the ratio of the mode quality factor to the mode volume. In  
84 addition, the spontaneous emission becomes directional; the photons emit-  
85 ted into the nicely shaped cavity mode can be more easily coupled into  
86 downstream optical components.

87 By embedding InGaAs/GaAs quantum dots inside micropost mi-  
88 crocavities with quality (Q)-factors of around 1300 and Purcell factors  
89 around five, the properties of a single-photon source have been signifi-  
90 cantly improved.<sup>(7)</sup>; see Fig. 1. The probability of generating two pho-  
91 tons for the same laser pulse [estimated from  $g^2(0)$ ] can be as small as  
92 2% compared to a Poisson-distributed source (i.e., an attenuated laser)  
93 of the same mean photon rate, the duration of single-photon pulses  
94 is below 200 ps, and the sources emit identical (indistinguishable) pho-  
95 tons, as confirmed by two-photon interference in a Hong-Ou-Mandel  
96 type experiment.<sup>(7)</sup> Such sources have been employed to realize the  
97 BB84 QKD protocol, and to generate post-selected polarization-entangled  
98 photons.<sup>(8)</sup>

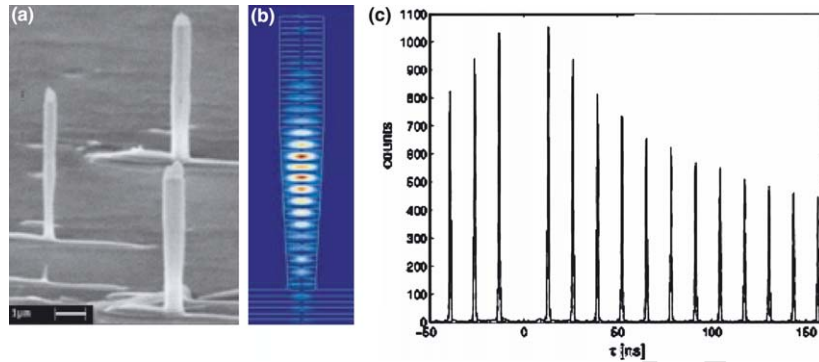


Fig. 1. (a) Scanning electron micrograph showing a fabricated array of GaAs/AlAs microposts ( $\sim 0.3\text{-}\mu\text{m}$  diameters,  $5\text{-}\mu\text{m}$  heights), with InAs/GaAs quantum dots embedded at the cavity center. (b) Electric field magnitude of the fundamental  $\text{HE}_{11}$  mode in a micropost microcavity with a realistic wall profile. (c) Photon correlation histogram for a single quantum dot embedded inside a micropost and on resonance with the cavity, under pulsed, resonant excitation. The histogram is generated using a Hanbury Brown and Twiss-type setup — the vanishing central peak (at  $\tau = 0$ ) indicates a large suppression of two-photon pulses (to  $\sim 2\%$  compared to a Poisson-distributed source, e.g., an attenuated laser, of the same intensity). The 13-ns peak-to-peak separation corresponds to the repetition period of excitation pulses.

99            These sources still face several great challenges, however. They require  
 100 cryogenic cooling ( $<10\text{ K}$ ), the output wavelengths are not yet readily tun-  
 101 able (present operation is around  $900\text{ nm}$ ), the out-coupling efficiency into  
 102 a single-mode traveling wave is still rather low ( $<40\%$ ),<sup>(9)</sup> and excitation  
 103 of quantum dots in microcavities presently requires *optical* pumping (elec-  
 104 trical pumping would be more desirable and efforts in that direction is  
 105 underway<sup>(6)</sup>). In the future, photonic crystal microcavities may lead to  
 106 much higher ratios of the quality factor and mode volumes, and there-  
 107 fore, much stronger cavity QED effects should be possible.<sup>(10)</sup> This would  
 108 enable an increase in the efficiency and speed of the single-photon devices,  
 109 and thus open the possibility for building integrated quantum informa-  
 110 tion systems. The spontaneous emission lifetime could be reduced further  
 111 to on the order of several picoseconds, which would allow the genera-  
 112 tion of single photons at a rate higher than  $10\text{ GHz}$ . Moreover, the Pur-  
 113 cell effect would also help in bringing the emitted photons closer to being  
 114 Fourier-transform limited in bandwidth. Finally, photonic-crystal based  
 115 cavities could even enable the realization of the strong coupling regime  
 116 with a single quantum dot exciton, opening the possibility for the genera-  
 117 tion of completely indistinguishable single photons by coherent excitation  
 118 schemes.

## 119 2.2. Other Single-emitter Approaches

120 Other isolated quantum system approaches to producing single pho-  
121 tons include isolated single fluorescence molecules<sup>(11)</sup> and isolated nitro-  
122 gen vacancies in diamond.<sup>(12)</sup> Two significant deficiencies of these sources  
123 for many applications is that it is not easy to efficiently out-couple the  
124 photons, and that the spectral spread of the light is typically quite large  
125 ( $\sim 120$  nm). This spectral width is non-optimal for applications relying on  
126 two-photon interference effects, and also for quantum cryptographic appli-  
127 cations (where one typically desires fairly narrow bandwidths to exclude  
128 background light).

129 More recently, single atoms<sup>(13)</sup> coupled to a high-finesse optical cavity  
130 have demonstrated features of single-photon operation. Despite their tech-  
131 nological challenges, this approach does offer the large potential advantage  
132 that the photons are emitted preferentially into the cavity modes, to which  
133 are easier to couple out of with couplings of 40–70% already achieved.  
134 Also, the frequency of the photons is necessarily matched to a strong  
135 atomic transition, which may allow for efficient quantum communication  
136 using photons, while other quantum information processing tasks, such as  
137 memory or state readout, are carried out in the atomic system.<sup>(14,15)</sup>

## 138 2.3. Downconversion Single-Photon Sources

139 Another effort toward single-photon sources relies on producing pho-  
140 tons in pairs, typically via the process of optical parametric down conver-  
141 sion (PDC).<sup>(16)</sup> The PDC process effectively takes an input photon from  
142 a pump beam and converts it into output pairs in a crystal possessing a  
143  $\chi^{(2)}$  nonlinearity. Thus the detection of one photon can be used to indi-  
144 cate (or herald) the existence of the second photon, which is available  
145 for further use. This second photon is, at low photon rates, left in an  
146 excellent approximation to a single-photon number state.<sup>(17)</sup> It has been  
147 demonstrated how these photons may then be converted into completely  
148 arbitrary quantum states with fidelities of 99.9%.<sup>(18)</sup> Recent efforts have  
149 focused on improving the collection of those pairs and improving the  
150 “single-photon accuracy,” e.g., the value of  $g^2(0)$ .

151 The physics of the PDC process guarantees that the output pairs will  
152 possess certain energy and momentum constraints, so that under appropri-  
153 ate conditions the detected location of the herald photon tightly defines  
154 the location of its twin, a significant advantage over other single-photon  
155 schemes. There have been many mode engineering efforts to improve this  
156 collection into a *single* mode,<sup>(19)</sup> but the current best collection efficiency is  
157 still only  $\sim 70\%$ . (Contrast this to the required single-photon efficiency of

158 over 99% for LOQC.)<sup>(4)</sup> One example of a promising method to improve  
 159 this is to directly modify the spatial emission profile of the photon pairs  
 160 (which are usually emitted along cones) so that the photons are emitted  
 161 preferentially into “beacon”-like beams, which couple more naturally into  
 162 single-mode optical fibers.<sup>(20)</sup> Another approach yet to be explored is the  
 163 use of adaptive optics to tailor the output modes. It should be noted that  
 164 not all quantum information processing applications require single-mode  
 165 performance; for example, free-space quantum key distribution is likely to  
 166 work nearly as well with a small number of modes.

167 Because the conversion of pump photons into pairs via PDC is a ran-  
 168 dom process, these sources suffer from the same problem that afflicts faint  
 169 laser sources—one cannot guarantee that one and only one photon-pair  
 170 is created at a time (i.e.,  $g^2(0) \neq 0$ ). Multiplexing and storage schemes  
 171 have been proposed to deal with this. They both work by similar princi-  
 172 ples (one scheme is based on space multiplexing<sup>(21)</sup>—see Fig. 2—and the  
 173 other is based on temporal multiplexing<sup>(22)</sup>)—photons are created at rela-  
 174 tively low rates where the probability of simultaneous multi-pair produc-  
 175 tion is low; contingent on the detection of a herald photon, the twin is  
 176 then “stored”, to be emitted in a controlled fashion at some later desired  
 177 time. The overall emission rate is reduced, but the rate of producing one  
 178 and only one photon at regular intervals is improved.

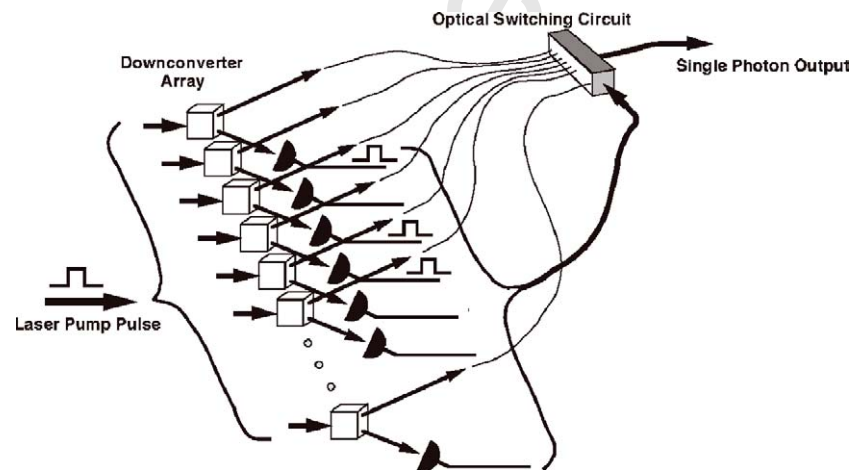


Fig. 2. Multiplexed PDC scheme to better approximate a source of single photons on demand. By operating an array of simultaneously pumped PDC sources at low photon production rates and optically switching the output of one of the PDC sources that did produce a photon to the single output channel, it is possible to increase the single-photon rate while maintaining a low rate of unwanted multiphoton pulses.

179 **3. ENTANGLED-PHOTON SOURCES**

180 Entangled states are now known to be a critical resource for realiz-  
 181 ing many quantum information protocols, such as teleportation and quan-  
 182 tum networking. An on-demand source of entangled photons would also  
 183 greatly aid the realization of all-optical quantum computing.

184 **3.1. Down-Conversion Schemes**

185 At present, by far the most prevalent source of entangled photon  
 186 pairs is parametric down conversion based on crystals with a  $\chi^{(2)}$  non-lin-  
 187 earity. As discussed above, it is precisely the temporal and spatial correla-  
 188 tions between the photon pairs which make them very promising for the  
 189 realization of an on-demand source of single photons. Much of the effort  
 190 in studying these sources has been devoted to the generation of *polariza-*  
 191 *tion*-entangled photon pairs, an area which has seen tremendous growth—  
 192 more than a million-fold improvement in the detected rates of polariza-  
 193 tion-entangled photons has been achieved in the past two decades (see  
 194 Fig. 3).

195 There are now several ways to realize polarization entanglement using  
 196 the PDC process. One method uses a single nonlinear crystal, cut for  
 197 “type-II” phase matching, and selecting out a particular pair of output  
 198 directions.<sup>(23)</sup> Although initially these sources used large gas lasers for  
 199 pumping, the recent availability of ultraviolet diode lasers has led to much

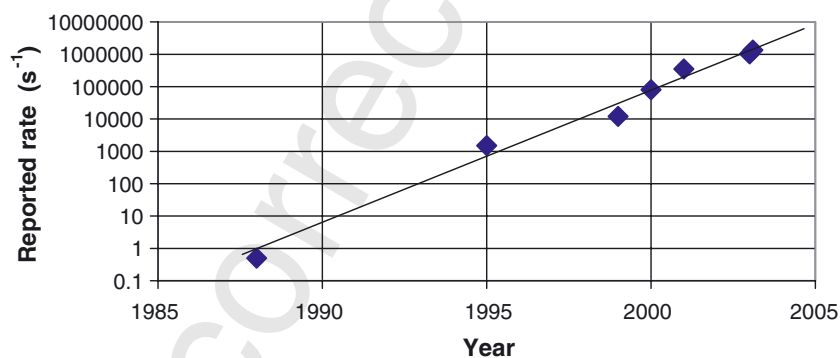


Fig. 3. The apparent “Moore’s Law” for entanglement. Shown are the reported detection rates of (polarization-)entangled photon pairs (from downconversion), as a function of year. The solid line—drawn to guide the eye—indicates the  $\times 100$  gain every 5 years. The primary limiting factor has now become the lack of single-photon counting detectors with saturation rates above 10 MHz.

200 more compact sources.<sup>(24)</sup> A potentially important disadvantage, in addi-  
201 tion to the need to compensate the birefringent walk-off with this scheme,  
202 is that the entanglement is present only over a particular pair of modes  
203 (corresponding to the intersection of two cones). One method to elimi-  
204 nate this disadvantage is to pump the crystal from two different direc-  
205 tions,<sup>(25,26)</sup> or to allow the PDC to occur in either of *two* crystals, the out-  
206 puts of which are superposed directly<sup>(27,28)</sup> or using a beam splitter.<sup>(29)</sup> By  
207 proper alignment, nearly all of the output modes can display polarization  
208 entanglement, which moreover is completely tunable.<sup>(30)</sup> Nearly perfect  
209 entanglement (within statistical uncertainty) has been observed with such  
210 sources. Results with short-pulse pumps<sup>(28,29,31)</sup> are encouraging, but the  
211 quality of the entanglement is typically not as high, a problem that will  
212 need to be addressed for future applications.

213 One disadvantage of all of these techniques is that the output spec-  
214 tral bandwidth is still quite wide (typically 1–10 nm) for possible coupling  
215 to atomic states. Research is underway to circumvent this problem by plac-  
216 ing the nonlinear crystals inside high finesse optical cavities, which signifi-  
217 cantly increases the probability of downconversion into a narrow spectral  
218 bandwidth.<sup>(14)</sup>

219 As discussed above, there are a number of approaches for improv-  
220 ing the coupling efficiency into single spatial modes. Improving conversion  
221 efficiency by finding higher non-linearity bulk crystals is limited by the  
222 choice of available crystals (with BBO and LiIO<sub>3</sub> being two of the better  
223 ones). Engineering crystals by processes such as periodic poling<sup>(32)</sup> allows  
224 one to take advantage of crystals (e.g., Lithium Niobate) with somewhat  
225 higher nonlinearities. The conversion efficiency into a specific mode can be  
226 further enhanced by some 1–2 orders of magnitude by creating waveguides  
227 in these crystals.<sup>(33)</sup> Because the waveguide is small, possibly even single  
228 mode, it can be much easier to collect the output light. However, the net  
229 outcoupling efficiencies achieved to date (10–20%) still require substantial  
230 improvement. Finally, by using a buildup cavity to recycle the unconverted  
231 pump photons, the effective conversion efficiency may be increased (at the  
232 expense of a more complicated setup).<sup>(34)</sup>

233 Entanglement in non-polarization degrees of freedom, such as  
234 energy/time-bin<sup>(35)</sup> and orbital angular momentum,<sup>(36)</sup> has also been real-  
235 ized recently. These may present some advantages over the polarization  
236 case, e.g., they allow implementation of higher-order quantum structures,  
237 such as qu-trits (3-level systems), and timing entanglement is more robust  
238 for transmission through optical fibers.

239 One problem plaguing all of these sources is that the production of  
240 pairs is a random process. By using short pulsed pumps, it is possible to  
241 define the times when *no* photon pairs will be produced, but there is still

242 no way to guarantee production of exactly one photon-pair during any  
243 given pulse. At least one theoretical scheme has been proposed to circum-  
244 vent this problem,<sup>(37)</sup> but practical implementations have yet to be realized.

### 245 3.2. $\chi^{(3)}$ -Nonlinearity Schemes

246 The difficulty of coupling the entangled photons into optical fibers  
247 has been overcome by directly producing them *inside* of the fiber, by  
248 exploiting the  $\chi^{(3)}$  (Kerr) nonlinearity of the fiber itself.<sup>(38)</sup> By placing  
249 the pump wavelength close to the zero-dispersion wavelength of the fiber,  
250 the probability amplitude for inelastic four-photon scattering can be sig-  
251 nificantly enhanced. Two pump photons at frequency  $\omega_p$  scatter through  
252 the Kerr nonlinearity to create simultaneous energy-time-entangled sig-  
253 nal and idler photons at frequencies  $\omega_s$  and  $\omega_i$ , respectively, such that  
254  $2\omega_p = \omega_s + \omega_i$ . Because of the isotropic nature of the Kerr nonlinearity  
255 in fused-silica-glass fibers, the correlated scattered photons are pre-  
256 dominantly co-polarized with the pump photons. Two such correlated  
257 down-conversion events from temporally multiplexed orthogonally polar-  
258 ized pumps can be configured to create polarization entanglement as well.  
259 In this way all four polarization-entangled Bell states have recently been  
260 prepared, violating Bell inequalities by up to ten standard deviations of  
261 measurement uncertainty.<sup>(39)</sup> One drawback is the existence of Raman  
262 scattering in standard optical fibers due to coupling of the pump photons  
263 with optical phonons in the fiber. However, for small pump-signal detun-  
264 ings the imaginary part of  $\chi^{(3)}$  in standard fibers is small enough that a  
265 10-fold higher probability of creating a correlated photon-pair in a suitable  
266 detection window can be obtained than the probability of two uncorre-  
267 lated Raman-scattered photons in the same detection window.<sup>(40)</sup> Further  
268 work to quantify Raman scattering at the single-photon level is needed.

### 269 3.3. Quantum Dot Entangled-photon Sources

270 A biexcitonic cascade from a semiconductor quantum dot might also  
271 allow the generation of polarization-entangled photon pairs on demand, since  
272 the selection rules should translate the anticorrelation of electron and hole  
273 spins in the biexcitonic state into polarization anticorrelation of photons.<sup>(41)</sup>  
274 However, this requires that the two decay paths from the biexcitonic state are  
275 indistinguishable; therefore, the effects such as dot anisotropy, strain, piezo-  
276 electric effects, and dephasing processes need to be minimized.<sup>(42)</sup> To accom-  
277 plish this, one needs to optimize quantum dot growth conditions and employ  
278 novel high-Q photonic crystal microcavities, which would increase the radiative  
279 recombination rate over the dephasing rate.<sup>(43)</sup>

## 280 4. SINGLE-PHOTON DETECTORS

281 As noted in the introduction, photon-based quantum information  
282 processing applications require that single photons, or more generally,  
283 the photon number in a multiphoton state, be detected with efficiency  
284 approaching unity. To that end much progress has been made in recent  
285 years towards developing high efficiency, low noise, and high count rate  
286 detectors, which can reliably distinguish the photon number in an incident  
287 quantum state.

### 288 4.1. Avalanche Devices

289 Detection of single photons with avalanche photodiodes<sup>(44)</sup> (APDs)  
290 biased above the breakdown voltage is convenient (no cryogenic temper-  
291 atures are needed) and relatively efficient. When one or more photons are  
292 absorbed, the generated carriers that undergo avalanche gain may cause a  
293 detectable macroscopic breakdown of the diode p–n junction. APD pho-  
294 ton counters suffer both from dark counts, where thermally generated  
295 charge carriers cause a detection event, and from after-pulses, where carri-  
296 ers from a previous avalanche cause subsequent detection events when the  
297 APD is reactivated.

298 The best counters at visible wavelengths have been made with sili-  
299 con APDs. These work well because of both the material system's abil-  
300 ity to provide very low-noise avalanche gain and the availability of silicon  
301 of nearly perfect quality. For example, the single photon-counting mod-  
302 ules (SPCMs), made by Perkin-Elmer (SPCM-AQR-16), can have 50–70%  
303 quantum efficiency near 630-nm wavelength, < 25 dark count/s, and can  
304 count at rates up to 10–15 MHz.<sup>†, (45)</sup> The dark-count rate is low enough  
305 for the SPCMs to be operated continuously except for a 50-ns avalanche  
306 quench time, although heating effects limit the CW counting rate to about  
307 5 MHz. After-pulsing is less than 0.5%. The quantum efficiency of the  
308 SPCMs drops at longer wavelengths (2% at 1  $\mu\text{m}$ ). Attempts to resolve  
309 multiple photons by splitting a multi-photon pulse into several time bins  
310 (e.g., with a storage loop) have been made, but they are limited by losses  
311 in the device switching photons into and out of the loop, and by the  
312 non-unity detector efficiencies.<sup>(46)</sup>

---

<sup>†</sup>Certain trade names and company products are mentioned in the text in order to specify adequately the experimental procedure and equipment used. In no case does such identification imply recommendation or endorsement by the National Institute of Standards and Technology, nor does it imply that the products are necessarily the best available for the purpose.

313 The Visible Light Photon Counter<sup>(47)</sup> (VLPC) and Solid State Photo-  
 314 multiplier<sup>(48)</sup> (SSPM) are modified Si devices which operate using a spa-  
 315 tially localized avalanche from an impurity band to the conduction band.  
 316 They possess high quantum efficiency (estimated to be  $\sim 95\%$ ) with low  
 317 multiplication noise. The localized nature of the avalanche allows high effi-  
 318 ciency photon-number discrimination,<sup>(49)</sup> which is not possible with con-  
 319 ventional APDs. Using this capability the non-classical nature of PDC  
 320 has been investigated and violations of classical statistics demonstrated.<sup>(50)</sup>  
 321 Unfortunately, these detectors require cooling to 6 K for optimal perfor-  
 322 mance, and even then they display dark count rates in excess of  $10^3 \text{ s}^{-1}$ .

323 In the infrared, 1–1.6  $\mu\text{m}$ , the best results to date have come from  
 324 APDs having InGaAs as the absorption region that is separate from a  
 325 multiplication layer of InP.<sup>(51)</sup>; see Fig.4. This has proven to be a bet-  
 326 ter solution than germanium APDs.<sup>(52)</sup> To suppress the high dark count  
 327 rate in these devices, at best thousands of times worse than in sili-  
 328 con APDs, cooled InGaAs/InP APDs are usually activated for only  $\sim 1$ –  
 329 10 ns duration to coincide with the arrival of the photon to be detected.  
 330 The reported quantum efficiencies are typically between 10–30%, and the

COLOR ON WEB

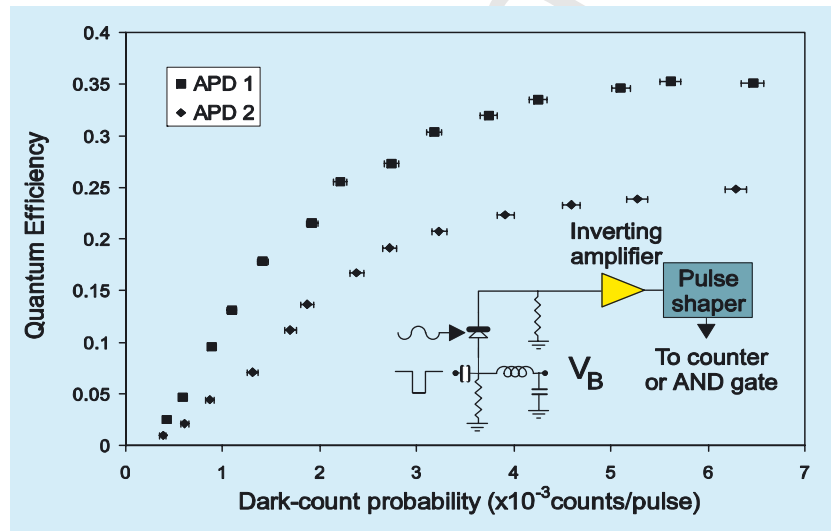


Fig. 4. Quantum efficiency versus dark-count probability for two InGaAs APDs operated in gated Geiger mode near 1537 nm wavelength. In the gated Geiger mode, the APD is biased below breakdown and a short electrical pulse ( $\sim 1$  ns), coincident with the incident light pulse containing the photon to be detected, brings it momentarily into the breakdown region. The inset shows a schematic of the electronic circuit used with the APDs (from Ref. 38).

331 APDs are usually operated at a count rate of 100 kHz in order to allevi-  
332 ate after-pulsing caused by carriers trapped between the InGaAs and InP  
333 layers.

#### 334 4.2. Superconducting Devices

335 Superconducting devices offer the potential to achieve levels of perfor-  
336 mance that exceed those of conventional semiconductor APDs. Although  
337 there are many types of superconducting detectors, only three have been  
338 used to observe single optical photons: the transition-edge sensor<sup>(53)</sup>  
339 (TES), the superconducting tunnel junction<sup>(54)</sup> (STJ), and the supercon-  
340 ducting single photon detector (SSPD).<sup>(55)</sup> Both the TES and the STJ  
341 detectors have been able to detect single photons and count the number  
342 of photons absorbed by the detector. The TES detector uses the steep  
343 slope of the resistance as a function of temperature at the superconduct-  
344 ing transition as a very sensitive thermometer. This thermometer is able to  
345 measure the temperature change in an absorber when one or more pho-  
346 tons are absorbed (see Fig. 5). The TES detectors are slow, capable of  
347 count rates at most up to 100 kHz, but essentially have no dark counts.<sup>(53)</sup>  
348 The reported detection efficiency currently varies from 20 to 40% in the  
349 telecom to optical band, although significant improvements in detection  
350 efficiency and speed are being realized with better detector designs (e.g.,  
351 anti-reflection coatings) and research into new superconducting materials.

352 In an STJ detector, excitations of the superconductor are generated  
353 when a photon is absorbed. The excited quasiparticles can create an  
354 enhanced tunneling current which is proportional to the energy of the  
355 photon (or the number of photons absorbed). These detectors are similar  
356 in speed to the TES and also have no dark counts. The detection efficiency  
357 demonstrated to date is roughly 40% for visible photons,<sup>(54)</sup> which could  
358 be improved with AR coatings.

359 The SSPD detectors are extremely fast detectors (~100-ps total pulse  
360 duration) that have single photon sensitivities.<sup>(55)</sup> In an SSPD, the detec-  
361 tor is a narrow superconducting current path on a substrate. This path is  
362 current-biased at a point just below the superconducting critical current. A  
363 local hot spot is formed where a photon(s) is absorbed, locally destroying  
364 the superconductivity. This forces the current to flow around the hot spot  
365 causing the current density around the hot-spot to exceed the critical cur-  
366 rent density. As a result, the device develops a resistance, causing a voltage  
367 to appear across the device. These detectors are single-photon-threshold  
368 devices and are not able to resolve the photon number in multiphoton  
369 pulses. Typical implementations use meandering paths to increase the sen-  
370 sitive area, which is otherwise very small due to the narrowness required

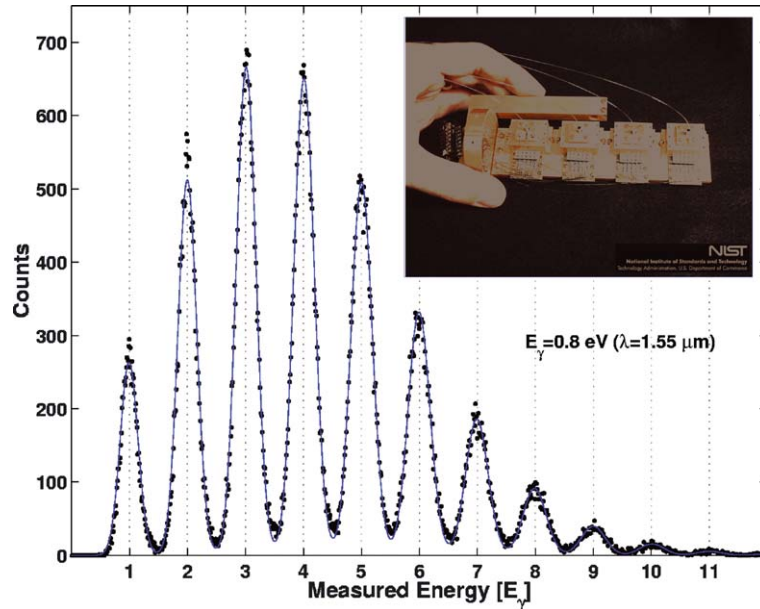


Fig. 5. Measured Poisson photon-number distribution of an attenuated, pulsed 1550-nm laser, repeatedly measured using a TES. The TES devices are made of superconducting tungsten and operated at a temperature of 100 mK. The horizontal axis is the pulse height of the photon absorption events in units of the energy of one 1550-nm photon, 0.8 eV (from Ref. 53). The inset shows a photograph of four fiber-coupled devices prepared to be cooled to 100 mK.

371 for the conducting path. Much improvement in device fabrication and  
 372 design is needed to improve the quantum efficiencies of these devices  
 373 beyond the current values of  $\sim 20\%$ ; the detection efficiency is lower still,  
 374 due to the area effect mentioned above.

#### 375 4.3. Frequency Upconversion

376 Detection techniques based on frequency upconversion allows IR  
 377 photons to be converted into the visible where single photon detection is  
 378 more efficient and convenient. Frequency upconversion uses sum-frequency  
 379 generation in a non-linear optical crystal to mix a weak input signal  
 380 at  $\omega_{\text{in}}$  with a strong pump at  $\omega_{\text{p}}$  to yield a higher-frequency output  
 381 field at  $\omega_{\text{out}} = \omega_{\text{in}} + \omega_{\text{p}}$ . With sufficient pump power this upconversion  
 382 can occur with near unity efficiency even for weak light fields at the  
 383 single-photon level. For LOQC and quantum key distribution applications,

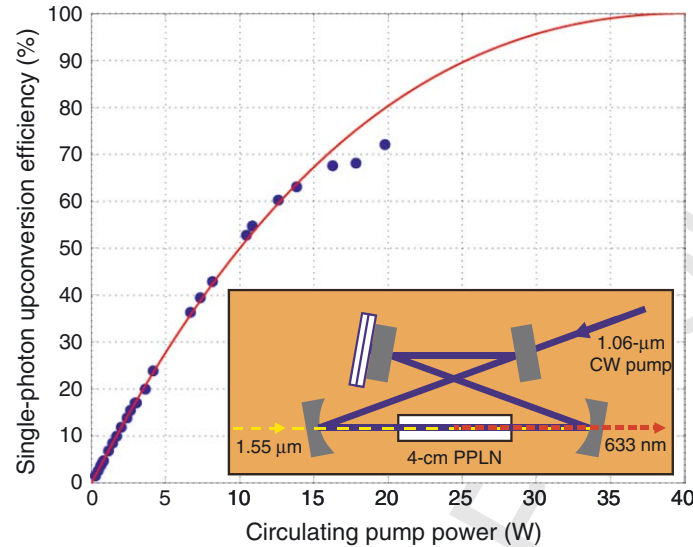


Fig. 6. CW single-photon upconversion efficiency versus circulating pump power in the pump enhancement ring cavity (inset). Solid line is a theoretical fit to data. At high pump powers lower than expected efficiencies is due to heating in PPLN that caused thermal instability in the ring cavity lock. See Ref. 56 for results with improved cavity lock.

384 telecommunication-wavelength photons at  $1.55 \mu\text{m}$  can then be efficiently  
 385 detected with low-noise, high quantum-efficiency Si APDs. Recently, up-  
 386 conversion of single photons from  $1.55$  to  $0.63 \mu\text{m}$  in bulk periodically  
 387 poled lithium niobate (PPLN) has been demonstrated with an efficiency of  
 388  $90\%$ ,<sup>(56)</sup> limited only by the available continuous wave (CW) pump power  
 389 at  $1.06 \mu\text{m}$ . See Fig. 6. The bulk PPLN crystal is embedded inside a pump  
 390 enhancement cavity that also imposes a well-defined spatial mode for the  
 391 single-pass input photons. One approach to eliminate the need for a stabil-  
 392 ized buildup cavity is to use a bright pulsed escort beam which is tem-  
 393 porally mode-matched to the input photon. Such a system has enabled  
 394 single-photon conversion efficiencies of  $\sim 80\%$  and backgrounds less than  
 395  $10^{-3}$  per pulse.<sup>(57)</sup>

396 The pump power requirement can be relaxed by using a waveguide  
 397 PPLN crystal,<sup>(58)</sup> but the effect of waveguide losses must be addressed  
 398 to achieve the required near-unity net upconversion efficiency. The next  
 399 step is to demonstrate frequency upconversion of a quantum state,<sup>(59)</sup> i.e.,  
 400 high fidelity frequency translation of a single photon in an arbitrary quan-  
 401 tum polarization state. This will allow a modular approach to developing  
 402 LOQC technologies. For example, the photonic qubits and ancilla photons

403 can be prepared at wavelengths with the most convenient and efficient  
404 methods, and then converted with near unit efficiency to wavelengths that  
405 are optimal for photonic logic gates employing quantum interference. Sim-  
406 ilarly, tunable quantum frequency upconversion can be used to match the  
407 required wavelengths to the resonant transitions in various atomic systems,  
408 for applications such as quantum repeaters.<sup>(14)</sup> As another example, there  
409 have also been proposals<sup>(15)</sup> to couple the photons to an atomic vapor sys-  
410 tem—the excitation of a single atom can be made very probable by having  
411 many atoms, and that excitation can be read out with very high efficiency  
412 by using a cycling transition. Such schemes could potentially yield efficien-  
413 cies in excess of 99.9%. However, there are critical noise issues which must  
414 still be addressed.

## 415 5. CONCLUSIONS

416 Though tremendous progress has been achieved, more development  
417 is clearly necessary to bring these technologies to the level of opera-  
418 tion needed for LOQC. Nevertheless, already they have shown promise,  
419 enabling the realization of simple quantum gates, and improved quan-  
420 tum key distribution protocols. We anticipate that further improvements  
421 over the next few years will continue to make optical qubits an attrac-  
422 tive system, though it remains to be seen whether the extremely demand-  
423 ing LOQC requirements can be met.

## 424 ACKNOWLEDGMENTS

425 P. Kumar and F. Wong would like to acknowledge support of the  
426 MURI Center, for Quantum Information Technology: Entanglement, Tele-  
427 portation, and Quantum Memory (ARO program DAAD19-00-1-0177);  
428 P. Kwiat, A. Migdall, Sae Woo Nam and J. Vuckovic would like to  
429 acknowledge support by the MURI Center for Photonic Quantum Infor-  
430 mation Systems (ARO/ARDA program DAAD19-03-1-0199). A. Midgall  
431 would also like to acknowledge DARPA/QUIST support.

## 432 REFERENCES

- 433 1. N. Gisin *et al.*, *Rev. Modern Phys.* **74**, 145 (2002).
- 434 2. A. Migdall, *Phys. Today* (January, 1999), 41.
- 435 3. S. J. van Enk *et al.*, *J. Mod. Opt.* **44**, 1727 (1997); J. I. Cirac, A. K. Ekert, S. F. Huelga,  
436 and C. Macchiavello, *Phys. Rev. A* **59**, 4249 (1999); H. Buhrman, R. Cleve, and W. van

- 437 Dam, *SIAM J. Comput.* **30**, 1829 (2001).  
 438 4. E. Knill, R. Laflamme, and G. J. Milburn, *Nature* **409**, 46 (2001).  
 439 5. P. Michler *et al.*, *Science* **290**, 2282 (2000); C. Santori *et al.*, *Phys. Rev. Lett.* **86**, 1502  
 440 (2001).  
 441 6. Z. Yuan *et al.*, *Science* **295**, 102 (2002).  
 442 7. J. Vuckovic *et al.*, *Appl. Phys. Lett.* **82**, 3596 (2003); C. Santori *et al.*, *Nature* **419**, 594  
 443 (2002).  
 444 8. E. Waks *et al.*, *Nature* **420**, 762 (2002); D. Fattal *et al.*, to appear in *Phys. Rev. Lett.*  
 445 (2004). ■  
 446 9. M. Pelton *et al.*, *Phys. Rev. Lett.* **89**, 233602 (2002).  
 447 10. J. Vuckovic and Y. Yamamoto, *Appl. Phys. Lett.*, **82**, 2374 (2003).  
 448 11. L. Brunel, B. Lounis, P. Tamarat, and M. Orrit, *Phys. Rev. Lett.* **83**, 2722 (1999).  
 449 12. C. Kurtsiefer, S. Mayer, P. Zarda, and H. Weinfurter, *Phys. Rev. Lett.* **85**, 290 (2000);  
 450 R. Brouri *et al.*, *Eur. Phys. J. D* **18**, 191 (2002).  
 451 13. A. Kuhn, M. Hennrich, and G. Rempe, *Phys. Rev. Lett.* **89**, 067901 (2002); J. McKeever  
 452 *et al.*, to appear in *Science* (Feb. 2004). ■  
 453 14. J. H. Shapiro, *New J. Phys.* **4**, 47.1 (2002).  
 454 15. A. Imamoglu, *Phys. Rev. Lett.* **89**, 163602 (2002); D. F. V. James and P. G. Kwiat, *Phys.*  
 455 *Rev. Lett.* **89**, 183601 (2002).  
 456 16. D. C. Burnham and D. L. Weinberg, *Phys. Rev. Lett.* **25**, 84 (1970).  
 457 17. C. K. Hong and L. Mandel, *Phys. Rev. Lett.* **56**, 58 (1986).  
 458 18. N. Peters *et al.*, *Quant. Inform and Comput.* **3**, 503–517 (2003).  
 459 19. C. Kurtsiefer, M. Oberparleiter, and H. Weinfurter, *Phys. Rev. A* **64**, 023802 (2001);  
 460 F. A. Bovino *et al.*, *Opt. Commun.* **227**, 343 (2003).  
 461 20. S. Takeuchi, *Opt. Lett.* **26**, 843 (2001).  
 462 21. A. L. Migdall, D. Branning, and S. Castelletto, *Phys. Rev. A* **66**, 053805 (2002).  
 463 22. T. B. Pittman, B. C. Jacobs, and J. D. Franson, *Phys. Rev. A* **66**, 42303 (2002);  
 464 P. G. Kwiat *et al.*, *Proc. SPIE* **5161**, 87 (2004).  
 465 23. P. G. Kwiat *et al.*, *Phys. Rev. Lett.* **75**, 4337 (1995).  
 466 24. P. Trojek, Ch. Schmid, M. Bourennane and H. Weinfurter, *Opt. Exp.* **12**, 276 (2004).  
 467 25. D. Branning, W. Grice, R. Erdmann, and I. A. Walmsley, *Phys. Rev. A* **62**, 013814  
 468 (2000).  
 469 26. M. Fiorentino *et al.*, quant-ph/0309071; to appear in *Phys. Rev. A*  
 470 27. P. G. Kwiat *et al.*, *Phys. Rev. A* **60**, R773 (1999).  
 471 28. G. Bitton, W. P. Grice, J. Moreau, and L. Zhang *Phys. Rev. A* **65**, 063805 (2002).  
 472 29. Y. -H. Kim *et al.*, *Phys. Rev. A* **63**, 062301 (2001).  
 473 30. A. G. White, D. F. V. James, P. H. Eberhard, and P. G. Kwiat, *Phys. Rev. Lett.* **83**, 3103  
 474 (1999).  
 475 31. Y. Nambu *et al.*, *Phys. Rev. A* **66**, 033816 (2002); B.-S. Shi and A. Tomita, *Phys. Rev. A*  
 476 **69**, 013803 (2004).  
 477 32. S. Tanzilli *et al.*, *Electron. Lett.* **37**, 26 (2001); C. E. Kuklewicz *et al.*, *Phys. Rev. A* **69**,  
 478 013807 (2004).  
 479 33. K. Banaszek, A. B. U'Ren, and I. A. Walmsley, *Opt. Lett.* **26**, 1367 (2001); K. Sanaka,  
 480 K. Kawahara, and T. Kuga, *Phys. Rev. Lett.* **86**, 5620 (2001).  
 481 34. M. Oberparleiter and H. Weinfurter, *Opt. Commun.* **183**, 133 (2000).  
 482 35. I. Marcikic *et al.*, *Phys. Rev. A* **66**, 062308 (2002).  
 483 36. A. Mair, A. Vaziri, G. Weihs, and A. Zeilinger, *Nature* **412**, 312 (2001); N. K. Langford,  
 484 quant-ph/0312072.  
 485 37. T. B. Pittman *et al.*, in *IEEE J. Selec. Top. Quant. Electron.*, special issue on “Quantum  
 486 Internet Technologies” (2003).

- 487 38. M. Fiorentino, P. L. Voss, J. E. Sharping, and P. Kumar, *IEEE Photonics Tech. Lett.* **14**,  
488 983 (2002).
- 489 39. X. Li, P. Voss, J. E. Sharping, and P. Kumar, Quant. Electr. and Laser Science Conf.,  
490 Baltimore, MD, June 1–6, 2003, paper QTuB4 in QELS’03 Technical Digest (Optical  
491 Society of America, Washington, D.C. 2003); *ibid*, quant-ph/0402191.
- 492 40. P. L. Voss and P. Kumar, *Opt. Lett.* **29**, 445 (2004).
- 493 41. O. Benson, C. Santori, M. Pelton, and Y. Yamamoto, *Phys. Rev. Lett.* **84**, 2513 (2000).
- 494 42. C. Santori *et al.*, *Phys. Rev. B* **66**, 045308 (2002).
- 495 43. J. Vuckovic and Y. Yamamoto, *Appl. Phys. Lett.* **83**, 2374 (2003).
- 496 44. W. G. Oldham, R. R. Samuelson, and P. Antognetti, *IEEE Trans. Electron. Dev.* **ED-19**,  
497 1056 (1972).
- 498 45. <http://optoelectronics.perkinelmer.com/>
- 499 46. M. J. Fitch, B. C. Jacobs, T. B. Pittman, and J. D. Franson, *Phys. Rev. A* **68**, 043814  
500 (2003); D. Achilles *et al.*, *Opt. Lett.* **28**, 2387 (2003); J. Rehacek *et al.*, quant-ph/0303032  
501 (2003).
- 502 47. E. Waks, K. Inoue, E. Diamanti, and Y. Yamamoto, quant-ph/0308054 (2003).
- 503 48. P. G. Kwiat *et al.*, *Appl. Opt.* **33**, 1844 (1994).
- 504 49. J. Kim, S. Takeuchi, Y. Yamamoto, and H. H. Hogue, *Appl. Phys. Lett.* **74**, 902 (1999).
- 505 50. E. Waks *et al.*, quant-ph/0307162 (2003).
- 506 51. A. Lacaita, F. Zappa, S. Cova, and P. Lovati, *Appl. Opt.* **35**, 2986 (1996); G. Ribordy,  
507 J.-D. Gautier, H. Zbinden, and N. Gisin, *Appl. Opt.* **37**, 2272 (1998); P. A. Hiskett,  
508 G. S. Buller, A. Y. Loudon, J. M. Smith, Ivair Gontijo, Andrew C. Walker, Paul D.  
509 Townsend, and Michael J. Robertson, *Appl. Opt.* **39**, 6818 (2000); J. G. Rarity, T. E. Wall,  
510 K. D. Ridley, P. C. M. Owens, and P. R. Tapster, *Appl. Opt.* **39**, 6746 (2000); N. Namek-  
511 ata, Y. Makino, S. Inoue, *Opt. Lett.* **27**, 954 (2002); A. Tomita and K. Nakamura, *Opt.*  
512 *Lett.* **27**, 1827 (2002); D. S. Bethune, W. P. Risk, and G. W. Pabst, quant-ph/03111120  
513 (2003); P. L. Voss, K. G. Köprülü, S.-K. Choi, S. Dugan, and P. Kumar, “14-MHz rate  
514 photon counting with room temperature InGaAs/InP avalanche photodiodes,” *J. Mod.*  
515 *Opt.* (2004), to appear.
- 516 52. A. Lacaita, P. A. Francese, F. Zappa, and S. Cova, *Appl. Opt.* **33**, 6902 (1994).
- 517 53. A. J. Miller, S. W. Nam, J. M. Martinis, and A. V. Sergienko, *Appl. Phys. Lett.* **83**, 791  
518 (2003).
- 519 54. A. Peacock *et al.*, *J. Appl. Phys.* **81**, 7641 (1997).
- 520 55. G. N. Gol’tsman *et al.*, *Appl. Phys. Lett.* **79**, 705 (2001).
- 521 56. M. Albota and F. N. C. Wong, to appear in *Opt. Lett.* (2004).
- 522 57. A. VanDevender and P. G. Kwiat, to appear in *J. Mod. Opt.* (2004).
- 523 58. K. R. Parameswaran *et al.*, *Opt. Lett.* **27**, 179 (2002).
- 524 59. J. M. Huang and P. Kumar, *Phys. Rev. Lett.* **68**, 2153 (1992).